Supplemental Materials for

Transition from Sign-reversed to Sign-preserved Cooper-pairing Symmetry in Sulfur-doped Iron Selenide Superconductors

Qisi Wang, J. T. Park*, Yu Feng, Yao Shen, Yiqing Hao, Bingying Pan, J. W. Lynn, A. Ivanov, Songxue Chi, M. Matsuda, Huibo Cao, R. J. Birgeneau, D. V. Efremov, Jun Zhao†

Sample growth and characterizations

$K_xFe_{2-y}(Se_{1-z}S_z)_2$ (z = 0, 0.25, 0.4, 0.5) single crystals were synthesized by the self-flux method. The starting materials were high-purity K pieces, Fe powder, Se pieces and S powder with the nominal compositions [$K_{0.8}Fe_2(Se_{1-z}S_z)_2$ (z = 0, 0.25, 0.4, 0.5)]. The reaction mixtures were sealed in evacuated double-walled quartz ampoules and heated to 1030℃, and then slowly cooled to 730℃ within 100 hours before shutting off the power of the furnace. High quality single crystals with a mass of up to ~ 16 g were obtained by this technique. The superconducting properties of our single crystals were characterized with DC magnetic susceptibility and resistivity measurements on small pieces of crystals cut from large single crystals used for neutron scattering experiments (Fig. S1). The doping dependence of T_c is consistent with previous reports [1,2]. The lattice parameters and actual S concentrations were determined by neutron/X-ray diffraction refinements. Fig. S2 shows the diffraction pattern used for the refinement. We note that S doping should distribute almost equally into the 122 and 245 phases, since only one sets of lattice constants are observed (Table. S1).

Instrument configurations for the inelastic neutron scattering experiments

Our inelastic neutron scattering measurements were carried out on the HB3 and HB1 thermal triple-axis spectrometers at the High-Flux-Isotope Reactor (HFIR), Oak Ridge National Laboratory, United States, the IN8 thermal triple-axis spectrometer at the Institute Laue-Langevin, Grenoble, France, the PUMA thermal triple-axis spectrometer at the Heinz Maier-Leibnitz Zentrum (MLZ), Technische Universität München, Garching, Germany, and the BT-7 thermal triple-axis spectrometer at the NIST Center for Neutron Research (NCNR), United States. For all triple-axis (TAS) experiments, we used pyrolytic graphite [PG(002)] as monochromator and analyzer with the final neutron energy fixed at E_f = 14.7 meV. PG filters were used to eliminate the contamination from the higher-order neutrons and a correction has also been made for monitor contamination by higher-order neutrons. The z = 0 sample was measured on HB3. The z = 0.25 and z = 0.4 samples were measured on IN8. Additional data for the z = 0.25 sample were taken on HB1 [Fig. 3(i)]. The z = 0.5 sample was measured on BT-7 [Figs. 2(d), 3(d) and 3(h)] and PUMA [the inset of Fig. 2(d)]. The collimations of 48'- 80'- *sample* - 80'- 240', 48'- 80'- *sample* - 80'- 240' and *open* - 80'- sample - 80'- 120' were used on HB3, HB1 and BT-7, respectively. For IN8 and PUMA, both the monochromator and analyzer were double focused and no collimations were used. For all triple axis experiments, the energy resolution is about 1 meV at **Q** = (0.5, 0.75, 0) and E = 0 meV.

Momentum structure of the magnetic excitations and raw energy scans

To determine the detailed momentum structure of the magnetic excitations, we performed **Q**-scans along the H and K directions at E = 14 meV in the normal and superconducting states in the z = 0 sample. Each **Q**-scan can be fitted by a Gaussian peak on a linear background [Figs. S3, (a)-(d)]. The background subtracted data are presented in Figure 2. It is shown that the scattering is clearly anisotropic, with a significantly larger width along the H direction in both normal and superconducting states, which is consistent with earlier work [3]. The momentum anisotropy of the magnetic excitations persists in the z =

0.5 sample. As shown in Fig. S3(e), elliptically shaped magnetic response is also observed at $14 < E < 28$ meV.

Fig. S4 shows the raw energy scans measured in the superconducting state and normal state. The energy dependence of the intensity difference between the superconducting and the normal states presented in Figs. 3(a)-(d) were obtained by subtracting the normal state intensity from the superconducting state intensity (Fig. S3), and normalizing to the amplitude of the normal state **Q**-scans at similar energies between different doping levels.

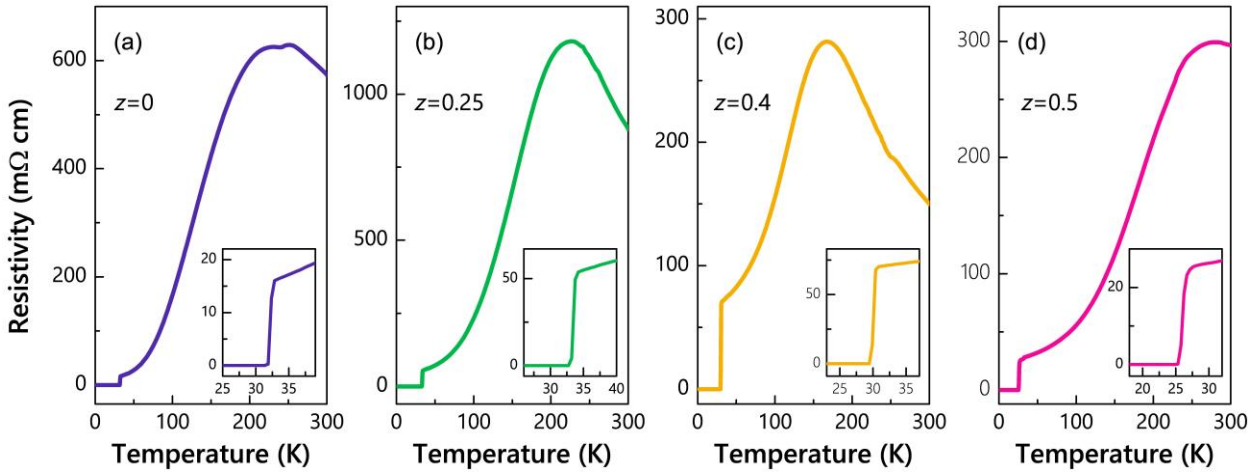

FIG. S1: Temperature dependence of resistivity of $K_xFe_{2-y}(Se_{1-z}S_z)_2$ (z = 0, 0.25, 0.4, 0.5) single crystals. (a)-(d) Temperature dependence of in-plane resistivity with different dopings. (a) z = 0; (b) z = 0.25; (c) z = 0.4; (d) z = 0.5. The insets show data around T_c on an enlarged scale.

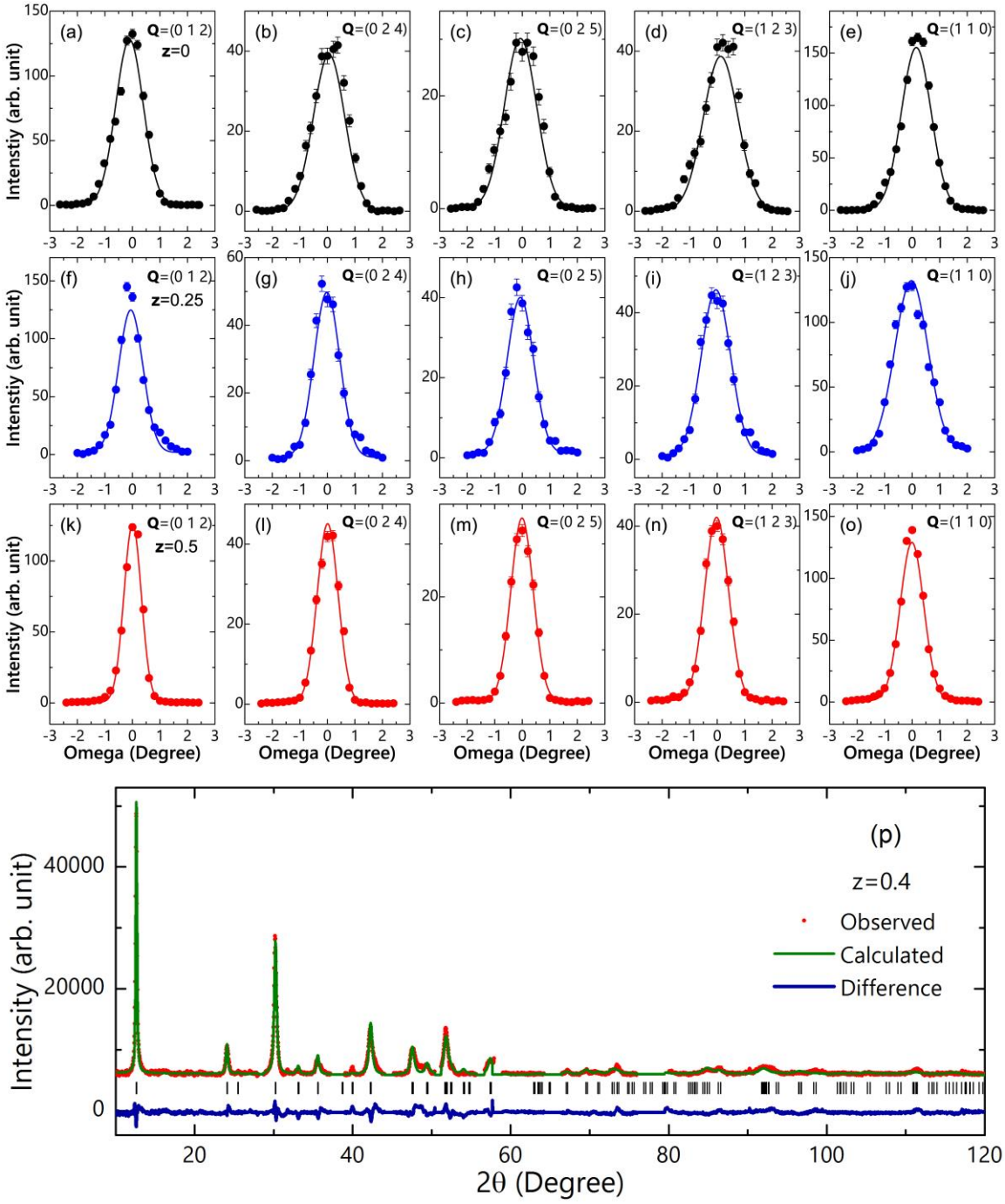

FIG. S2: Neutron and X-ray diffraction data. (a)-(o) Representative neutron diffraction pattern measured on single crystalline samples at the indicated dopings at 5 K. (a)-(e) z = 0; (f)-(j) z = 0.25; (k)-(o) z = 0.5. The filled circles and solid lines indicate observed and calculated intensities, respectively. About 100 similar nuclear Bragg peaks were used in our refinements for each doping. The measurements were performed on small pieces of single crystals cut from large single crystals used for inelastic neutron scattering experiments. (p) Observed (red) and calculated (green) X-ray powder diffraction intensities for z = 0.4 sample at 93 K. The missing data correspond to the strong reflections from the aluminum sample

environment at 93 K. The powder sample was obtained by grinding the single crystal used for the DC magnetic susceptibility measurements.

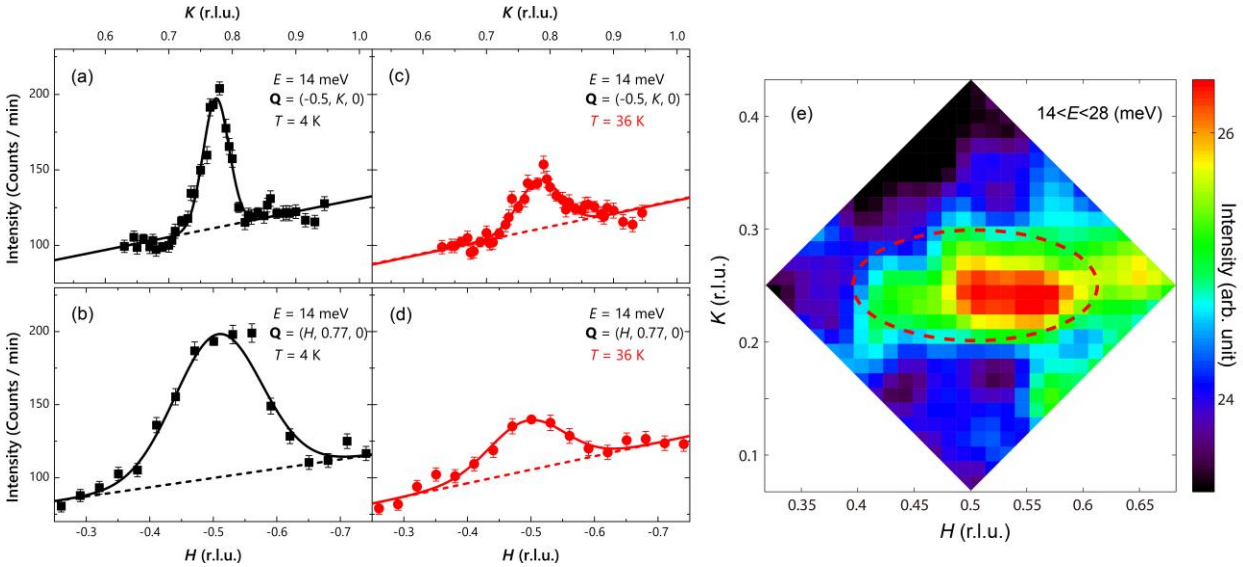

FIG. S3: Momentum structure of the magnetic excitations. (a)-(d) Raw **Q**-scans along the *K* and *H* directions at E = 14 meV at 4 K and 36 K in the z = 0 sample. The data can be fitted by a single Gaussian peak on a linear background. The dashed lines indicate the background. The error bars indicate one standard deviation. (e) Contour map of the magnetic excitations in the *HK* plane at 14 < E < 28 meV at T = 3 K in the z = 0.5 sample. The data of Fig. S2(e) was measured at the HRC time-of-flight chopper spectrometer at the Japan Proton Accelerator Research Complex (J-PARC), Tokai, Japan. An incident neutron energy of E_i = 102.4 meV was used and the single crystals were mounted with the incident neutron beam parallel to the *c* axis.

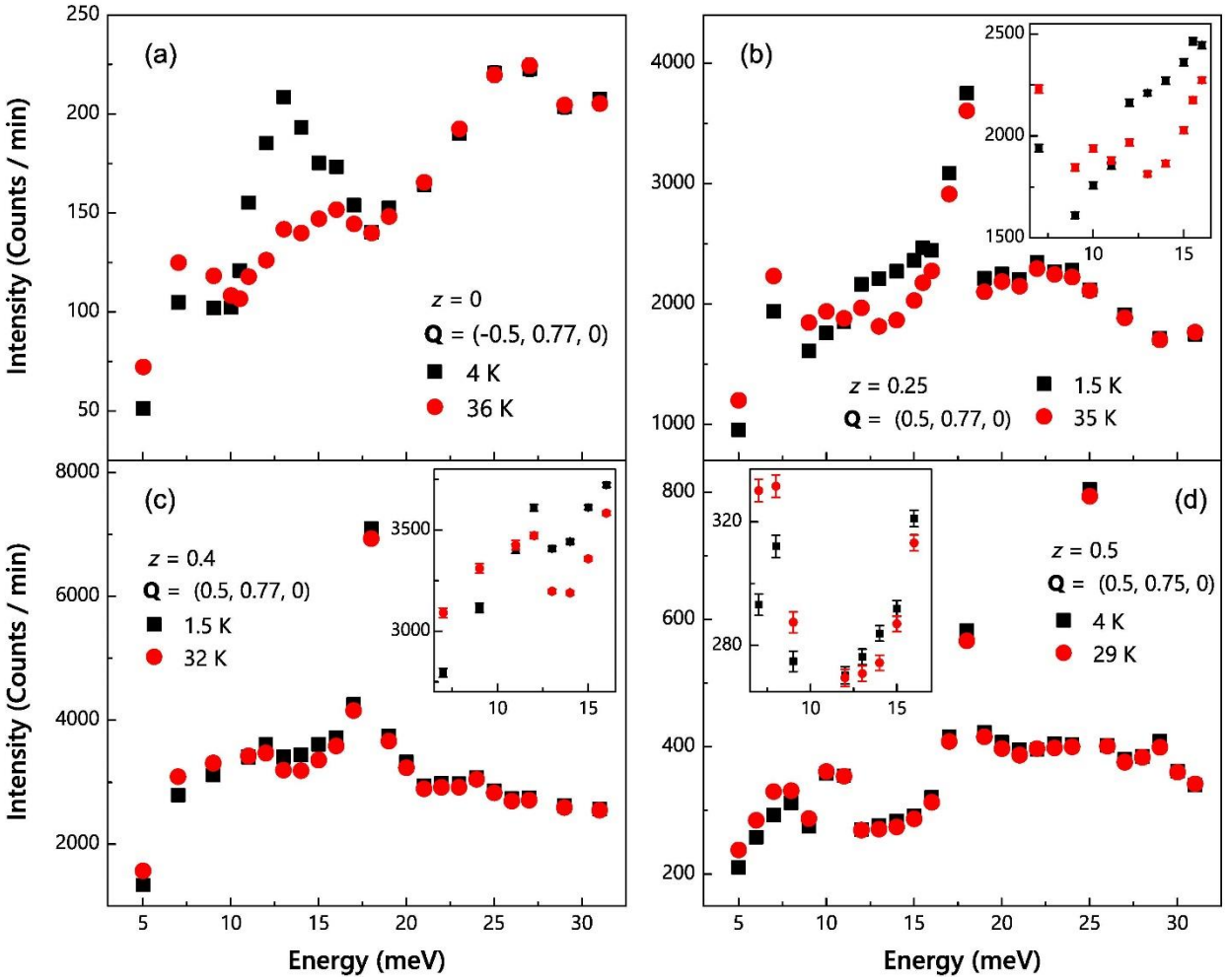

FIG. S4: Raw energy scans measured in the superconducting state (black) and the normal state (red). (a) z = 0; (b) z = 0.25; (c) z = 0.4; (d) z = 0.5. The insets show the data near the spin gap edge on an enlarged scale. To facilitate comparison of the resonance modes between different samples, E-scans in Fig. 3, (a)-(d) were normalized by the normal state magnetic excitation intensities. The error bars indicate one standard deviation.

Table. S1: Superconducting transition temperatures (T_c), refined structure parameters (1-Fe unit cell), and average chemical compositions of $K_xFe_{2-y}(Se_{1-z}S_z)_2$. The T_c is defined as the onset transition temperature in the magnetic susceptibility (Fig. 3), which is close to the zero-resistivity temperature (Fig. S1). Neutron diffraction measurements for the z = 0, z = 0.25 and z = 0.5 single crystals were performed at T = 5 K on the HB3A four-circle single-crystal diffractometer at the High-Flux Isotope Reactor at the Oak Ridge National Laboratory. Powder X-ray diffraction measurements of the z = 0.4 sample were performed at T = 93 K on a Bruker D8 Discover Diffractometer. We were not able to determine the Ch-Fe-Ch angles and Fe-Ch distances (Ch indicates chalcogenide atom) for z = 0.4 sample because of the low statistics of the powder X-ray diffraction data.

z (nominal)	a (Å)	c (Å)	x (refined)	2-y (refined)	z (refined)	Ch-Fe-Ch angles (°)	Fe-Ch distance (Å)	R_1	wRF^2	χ^2	T_c (K)
0	2.765(1)	7.026(4)	0.87(3)	1.62(2)	0	104.94(7)/111.78(12)	2.4654(16)	0.0449	0.0911	1.63	31.2
0.25	2.716(5)	6.968(3)	0.82(4)	1.66(3)	0.25(3)	104.4(3)/112.1(2)	2.430(3)	0.0469	0.0912	0.90	32.0
0.4	2.6993(8)	6.9677(1)	0.78(3)	1.60(3)	0.39(3)	-	-	0.0184	0.0257	7.03	28.4
0.5	2.687(3)	6.895(6)	0.82(3)	1.64(2)	0.50(2)	104.5(6)/112.0(12)	2.402(16)	0.0382	0.0751	1.43	25.4

*jitae.park@frm2.tum.de

† zhaoj@fudan.edu.cn

[1] K. Wang, H. Lei, C. Petrovic, *Phys. Rev. B* **84,** 054526 (2011).

[2] L. Li, Z. R. Yang, Z. T. Zhang, W. Tong, C. J. Zhang, S. Tan, Y. H. Zhang, *Phys. Rev. B* **84,** 174501 (2011).

[3] G. Friemel, W. P. Liu, E. A. Goremychkin, Y. Liu, J. T. Park, O. Sobolev, C. T. Lin, B. Keimer, D. S. Inosov, *Europhys. Lett.* **99,** 67004 (2012).